Opt Quant Electron (2011) 42:729–737
DOI 10.1007/s11082-011-9463-x

Analysis of ultrafast nonlinear phenomena's influences on output optical pulses and four-wave mixing characteristics in semiconductor optical amplifiers

S. R. Hosseini · M. Razaghi · N. K. Das

Received: 26 September 2010 / Accepted: 29 March 2011 / Published online: 16 April 2011

Abstract We have analysed the output pulse characteristics of semiconductor optical amplifier (SOA). It is shown that they can be modified due to the variation of input parameters, such as, gain, input pulsewidth, input pulse energy and effects imposed by the medium. Therefore, the influence of these parameters are analysed on the output pulse shape, spectrum, chirp and pulsewidth. We have used the nonlinear propagation equation taking into account the gain spectrum dynamics, gain saturation which depends on carrier depletion, carrier heating, spectral hole-burning, group velocity dispersion, self-phase modulation and two photon absorption. We have used the finite-difference beam propagation method to simulate the wave evolution both in time and spectral domain in the SOA. We have also simulated the four-wave mixing characteristics between pulses for various input pulses. An accurate output pulse shape can be achieved by controlling the mentioned parameters. To the authors knowledge, pulse shaping in co-propagation regime due to medium effect and input pulse shapes in presence of all nonlinear effects relevant to picosecond regime have been studied comprehensively, for the first time in this work.

Keywords Semiconductor optical amplifier · Finite-difference beam propagation method · Nonlinear effects · Four-wave mixing · Pulse shaping

1 Introduction

Currently, semiconductor optical amplifiers (SOAs) have significant practical interest in data communication applications, because of their small size, high optical gain, low input power

S. R. Hosseini · M. Razaghi (✉)
Department of Electrical and Computer Engineering, University of Kurdistan, P.O. Box: 416, Sanandaj, Iran
e-mail: m.razaghi@uok.ac.ir

N. K. Das
Electron Science Research Institute, Edith Cowan University, 270 Joondalup Drive, Joondalup, WA 6027, Australia

requirement, faster response time and large bandwidth (Aghajanpour et al. 2009; Rafailov et al. 2003; Razaghi et al. 2009a,b). Nonlinear effects are the basis of many schemes in ultrahigh-speed optical communication systems and devices, such as, all-optical modulators, demultiplexers and 3R regenerators that require very fast dynamics in fibre and semiconductor devices. SOA is one of the fundamental parts of the large-scale integration and nonlinear effects play an important role in pulse shaping process in it (Razaghi et al. 2009a,b).

The main objective of paper is to investigate, how the medium internal loss, input pulse-width and input energy affect the characteristics of the SOA's output pulse. To reach our goal, we have numerically simulated the optical wave propagation in the SOA. The beam propagation method (BPM) is widely used for the analysis of the field distribution in optical waveguides and optical pulse propagation in fibers (Agrawal and Olsson 1989). Based on the simulation time and results, we used the FD-BPM, because of short convergence time and excellent accuracy of the results (Razaghi et al. 2009a,b; Agrawal and Olsson 1989; Fernandez et al. 2006).

This paper is organized as follow; Sect. 1 is Introduction, Sect. 2 is Theory of the model, the equations which govern the dynamics of the amplification process, Sect. 3 is Simulation Results and Discussion and finally Conclusions are in Sect. 4.

2 Theory of the model

The model we have used is based on modified nonlinear Schrödinger equation, which explains the propagation of optical pulses in the SOA's medium (Das et al. 2000).

$$\begin{aligned}&\left[\frac{\partial}{\partial z}-\frac{i}{2}\beta_2\frac{\partial^2}{\partial\tau^2}+\frac{\gamma}{2}+\left(\frac{\gamma_{2p}}{2}+ib_2\right)|V(z,\tau)|^2\right]V(z,\tau)\\&=\left\{\frac{1}{2}g_N(\tau)\left[\frac{1}{f(\tau)}+i\alpha_N\right]+\frac{1}{2}\Delta g_T(\tau)\,(1+i\alpha_T)\right.\\&\quad\left.-i\frac{1}{2}\left.\frac{\partial g(\tau,\omega)}{\partial\omega}\right|_{\omega_0}\frac{\partial}{\partial\tau}-\frac{1}{4}\left.\frac{\partial^2 g(\tau,\omega)}{\partial\omega^2}\right|_{\omega_0}\frac{\partial^2}{\partial\tau^2}\right\}V(z,\tau)\end{aligned}\tag{1}$$

where, $V(z,\tau)$ is the complex envelope function of an optical pulse. The definitions of some parameters in the equation are as follow:

$$g_N(\tau)=g_0\exp\left[-\frac{1}{E_{sat}}\int_{-\infty}^{+\infty}u(s)\,|V(\tau-s)|^2\,ds\right]\tag{2}$$

$$f(\tau)=1+\frac{1}{\tau_{shb}P_{shb}}\int_{-\infty}^{\infty}u(s)\,e^{-s/\tau_{shb}}\,|V(\tau-s)|^2 ds\tag{3}$$

$$\begin{aligned}\Delta g_T(\tau)&=-h_1\int_{-\infty}^{+\infty}u(s)e^{-s/\tau_{ch}}\times(1-e^{-s/\tau_{shb}})\,|V(\tau-s)|^2\,ds\\&\quad-\mathrm{h}_2\int_{-\infty}^{+\infty}u(s)e^{-s/\tau_{ch}}\times(1-e^{-s/\tau_{shb}})\,|V(\tau-s)|^4\,ds\end{aligned}\tag{4}$$

$$\left.\frac{\partial g(\tau,\omega)}{\partial \omega}\right|_{\omega_0} = A_1 + B_1\left[g_0 - g(\tau,\omega_0)\right] \tag{5}$$

$$\left.\frac{\partial^2 g(\tau,\omega)}{\partial \omega^2}\right|_{\omega_0} = A_2 + B_2\left[g_0 - g(\tau,\omega_0)\right] \tag{6}$$

$$g(\tau,\omega_0) = g_N(\tau,\omega_0)/f(\tau) + \Delta g_T(\tau,\omega_0) \tag{7}$$

where, $\tau = t - z/v_g$ is the frame of local time which propagates with the group velocity of the optical pulse at central frequency. The slowly varying envelope function approximation is used in Eq. (1), where the temporal change of the complex envelope function is very slow compared with the cycle of an optical field. $|V(z,\tau)|^2$ represents the optical power of an optical pulse, β_2 is the group velocity dispersion (GVD), γ is linear loss, γ_{2p} is the two-photon absorption coefficient, $b_2(=\omega_0 n_2/cA)$ is the instantaneous self-phase modulation term due to the Kerr effect, n_2 is an instantaneous nonlinear refractive index, $\omega_0(=2\pi f_0)$ is the center angular frequency of the pulse, c is the velocity of light in vacuum, $A\ (=wd/\Gamma)$ is the effective area (d and w are the thickness and width of the active region, respectively, and Γ is the confinement factor). $g_N(\tau)$ is the saturated gain due to carrier depletion, g_0 is the linear gain, E_{sat} is the saturation energy, τ_s is the carrier lifetime, $f(\tau)$ is the spectral hole-burning function, P_{shb} is the spectral hole-burning saturation power, τ_{shb} is the spectral hole-burning relaxation time, α_N and α_T are the linewidth enhancement factor associated with the gain changes due to the carrier depletion and carrier heating, respectively. $\Delta g_T(\tau)$ is the resulting gain change due to the carrier heating and two-photon absorption, $u(s)$ is the unit step function, τ_{ch} is the carrier heating relaxation time, h_1 is the contribution of stimulated emission and free-carrier absorption to the carrier heating gain reduction, and h_2 is the contribution of two-photon absorption. Finally, A_1 and A_2 are the slope and the curvature of the linear gain at ω_0, respectively, while B_1 and B_2 are constants describing the changes in these quantities with saturation (Das et al. 2000; Hong et al. 1992).

As our model includes the dynamic gain change terms, i.e. the first- and second-order gain spectrum terms which are the last two terms of the right side in Eq. (1), we cannot separate the linear propagation term (GVD term) and phase compensation terms (other than GVD, first- and second-order gain spectrum terms). Hence, we have used the finite difference beam propagation method (FD-BPM) (Conte and de Boor 1981). If we replace the time derivative terms of Eq. (1) by the central-difference approximation Eq. (8) and integrate Eq. (1) with the small propagation step Δz, we obtain the tridiagonal simultaneous matrix Eq. (9),

$$\frac{\partial}{\partial\tau}V_k = \frac{V_{k+1} - V_{k-1}}{2\Delta\tau}, \quad \frac{\partial^2}{\partial\tau^2}V_k = \frac{V_{k+1} - 2V_k + V_{k-1}}{\Delta\tau^2} \tag{8}$$

$$\begin{aligned} &-a_k(z+\Delta z)V_{k-1}(z+\Delta z) + \{1 - b_k(z+\Delta z)\}V_k(z+\Delta z) \\ &-c_k(z+\Delta z)V_{k+1}(z+\Delta z) \\ &= \mathrm{a}_k(z)V_{k-1}(z) + \{1 + b_k(z)\}V_k(z) + c_k(z)V_{k+1}(z) \end{aligned} \tag{9}$$

where, $V_k = V(\tau_k)$, $V_{k+1} = V(\tau_k + \Delta\tau)$, $V_{k-1} = V(\tau_k - \Delta\tau)$ and $k = 1, 2, 3, \ldots, n$.

$$\mathrm{a}_k(z) = \frac{\Delta z}{2}\left[\frac{i\beta_2}{2\Delta\tau^2} + i\frac{1}{4\Delta\tau}\left.\frac{\partial g(\tau,\omega,z)}{\partial\omega}\right|_{\omega_0,\tau_k} - \frac{1}{4\Delta\tau^2}\left.\frac{\partial^2 g(\tau,\omega,z)}{\partial\omega^2}\right|_{\omega_0,\tau_k}\right] \tag{10}$$

$$\begin{aligned} \mathrm{b}_k(z) = -\frac{\Delta z}{2}\Bigg[&\frac{i\beta_2}{\Delta\tau^2} + \frac{\gamma}{2} + \left(\frac{\gamma_{2p}}{2} + ib_2\right)|V_k(z)|^2 - \frac{1}{2}g_N(\tau_k,\omega_0,z)(1+i\alpha_N) \\ &-\frac{1}{2}g_N(\tau_k,\omega_0,z)(1+i\alpha_T) - \frac{1}{2\Delta\tau^2}\left.\frac{\partial^2 g(\tau,\omega,z)}{\partial\omega^2}\right|_{\omega_0,\tau_k}\Bigg] \end{aligned} \tag{11}$$

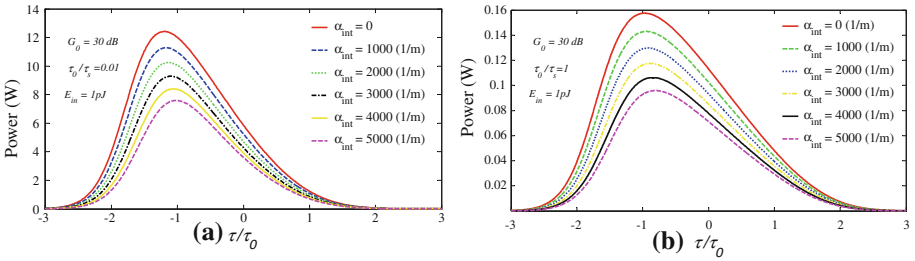

Fig. 1 The output pulse shape for several values of medium loss, for this case, the Gaussian input pulse energy and width are: **a** $E_{in} = 1\ pJ$, $\tau_0/\tau_s = 0.01$ and **b** $E_{in} = 1\ pJ$, $\tau_0/\tau_s = 1$. Output power decreases by increasing the internal losses

$$c_k(z) = \frac{\Delta z}{2}\left[\frac{i\beta_2}{2\Delta\tau^2} - i\frac{1}{4\Delta\tau}\frac{\partial g(\tau,\omega,z)}{\partial\omega}\bigg|_{\omega_0,\tau_k} - \frac{1}{4\Delta\tau^2}\frac{\partial^2 g(\tau,\omega,z)}{\partial\omega^2}\bigg|_{\omega_0,\tau_k}\right] \tag{12}$$

where, $\Delta\tau$ is the sampling time and n is the number of sampling. If we know $V_k(z)$, $(k = 1, 2, 3, \ldots, n)$ at position z, we can calculate $V_k(z + \Delta z)$ at position $z + \Delta z$ which is the propagation of a step Δz from position z, by using Eq. (9). It is not possible to directly calculate Eq. (9) because it is necessary to calculate the left-side terms $a_k(z + \Delta z)$, $b_k(z + \Delta z)$ and $c_k(z + \Delta z)$ of Eq. (10) from the unknown $V_k(z + \Delta z)$. Therefore, we have initially defined $a_k(z + \Delta z) \equiv a_k(z)$, $b_k(z + \Delta z) \equiv b_k(z)$ and $c_k(z + \Delta z) \equiv c_k(z)$ and obtained $V_k^{(0)}(z + \Delta z)$, as the zeroth order approximation of $V_k(z + \Delta z)$ by using Eq. (9). Then, we have substituted $V_k^{(0)}(z + \Delta z)$ in Eq. (9) and obtained $V_k^{(1)}(z + \Delta z)$ as the first-order approximation of $V_k(z + \Delta z)$ and finally obtained an accurate simulation results by iteration (Das et al. 2000).

3 Results and discussion

We have used the parameters of a bulk SOA (AlGaAs/GaAs, double heterostructure) with a wavelength of 0.86 μm in our simulation. The parameters are listed in Table 1 (Das et al. 2000). The following results are achieved, when the input pulses have sech^2 form and they are Fourier transform limited. The simulation results are verified by comparison with previously published works (Razaghi et al. 2009a). $G_0 = \exp(g_0 L)$ is an unsaturated single-pass amplifier gain, which is usually between 0 and 40 dB (Agrawal and Olsson 1989).

Figure 1 shows the output pulse shapes for several values of medium internal loss: (a) $E_{in} = 1\ pJ$, $\tau_0/\tau_s = 0.01$ and (b) $E_{in} = 1\ pJ$, $\tau_0/\tau_s = 1$. It has shown clearly that the temporal output pulse shapes in Fig. 1a are more asymmetric and compressed further, which is due to the effect of self-phase modulation (SPM). When the input pulsewidth is very shorter than the carrier lifetime, the leading edge of the pulse saturates the amplifier and the trailing edge experiences a lower gain, so the pulse shape becomes asymmetric. But in Fig. 1b, the input pulsewidth is equal to carrier lifetime. In this case, the trailing edge experiences approximately comparable gain to the leading edge and the pulse shape becomes more symmetric and broadened. Furthermore, when the internal loss of the SOA is increased, the output pulse power is decreased. But this relation is not linear. It has shown that the higher internal loss, leads to more symmetric output pulse shape. This is because the propagated pulse experiences lower influence by the saturation phenomena.

Table 1 List of parameters used in simulation Das et al. 2000

Symbol	Quantity	Value
L	SOA length	500 μm
A_r	Effective area	5 μm^2
f_o	Center frequency of the pulse	349 THz
β_2	Group velocity dispersion	0.05 $ps^2 cm^{-1}$
E_{sat}	Saturation energy	80 pJ
α_N	Linewidth enhancement factor due to the carrier depletion	3.1
α_r	Linewidth enhancement factor due to the carrier heating	2.0
h_1	The contribution of stimulated emission and free carrier absorption to the carrier heating gain reduction	0.13 $cm^{-1} pJ^{-1}$
h_2	The contribution of two photon absorption	126 fs $cm^{-1} pJ^{-2}$
τ_s	Carrier lifetime	200 ps
τ_{ch}	Carrier heating relaxation time	700 fs
τ_{shb}	Spectral -hole burning relaxation time	60 fs
P_{shb}	Spectral -hole burning relaxation power	28.3 W
γ	Linear loss	11.5 cm^{-1}
n_2	Instantaneous nonlinear Kerr effect	−0.70 cm^2 TW^{-1}
γ_{2p}	Two photon absorption coefficient	1.1 cm^{-1} W^{-2}
A_1		0.15 fs μm^1
A_2	Parameters describing second order Taylor	−80 fs
B_1	Expansion of the dynamically gain spectrum	−60 fs^2 μm^1
B_2		0 fs^2

Figure 2 shows the normalized spectrum of the output pulse shapes: (a) normalized spectrum corresponding to the pulse shapes shown in Fig. 1a, b normalized spectrum corresponding to the pulse shapes shown in Fig. 1b. It has shown that the output spectrum widths are broadened due to the increase of input pulsewidths. This effect has the same explanation described before, and it is mainly due to SPM. The oscillatory structures in the pulse spectra which is obvious in Fig. 2a, b, results from interference phenomena that is common to SPM in all nonlinear media (Agrawal and Olsson 1989). Moreover, the medium loss significantly shifts the spectrum (e.g. in the case of $E_{in} = 1\ pJ$, $\tau_0/\tau_s = 0.01$, there is 100 GHz shift for $\alpha_{int} = 0$ to $\alpha_{int} = 5000$ (1/m)).

Figure 3 shows the effect of input pulse and medium loss on the output pulse chirp ($\Delta\nu = -1/2\pi \times \partial\Phi/\partial t$) (Agrawal and Olsson 1989). The output chirp imposed by SOA is shown for: (a) $E_{in} = 1\ pJ$, $\tau_0/\tau_s = 0.01$ and (b) $E_{in} = 1\ pJ$, $\tau_0/\tau_s = 1$. Output chirp decreases for higher medium losses. It has shown in Fig. 3a, for picoseconds pulses, due to the effects of carrier depletion, negative chirp imposed to the entire amplified pulse. As the pulsewidth increases to tens of picoseconds negative chirp only imposed on the leading edge of the amplified pulse, but the trailing edge experiences positive chirp. This is because the gain can recover to its initial value.

In the following, we will study the width of output pulse. Figure. 4 shows: (a) the FWHM of output pulses for different values of unsaturated single pass gain (G_0) and (b): Normalized FWHM of the output pulses for different values of input pulse energies. It is shown that, when

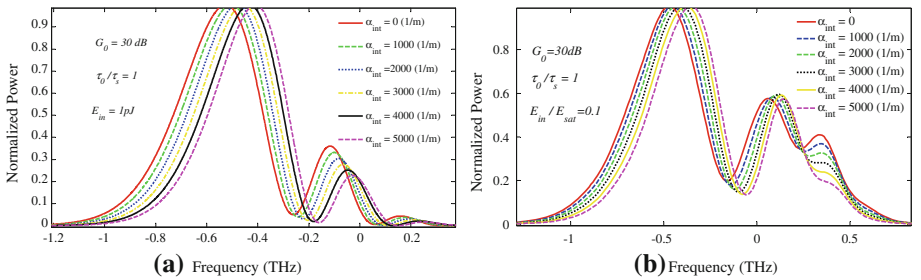

Fig. 2 The normalised output pulse spectrum corresponding to the pulse shapes that shown in Fig. 1. **a** Normalized spectrum corresponding to the pulse shapes shown in Fig. 1a. **b** Normalized spectrum corresponding to the pulse shapes shown in Fig. 1b. Medium loss causes a blue shift in spectrum

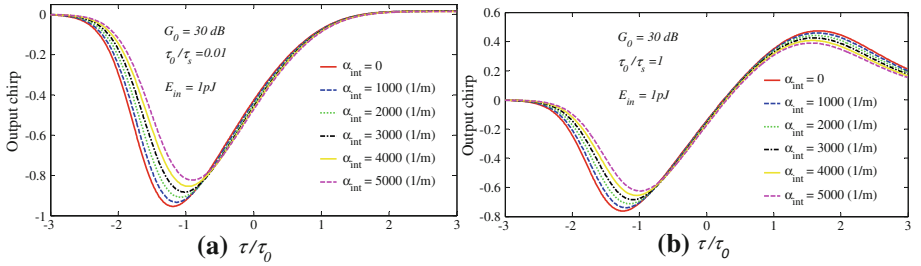

Fig. 3 The output pulse chirp for variety of medium loss values in the case of Gaussian input pulse. The energy and width of input pulse are : **a** $E_{in} = 1\ pJ$, $\tau_0/\tau_s = 0.01$ and **b** $E_{in} = 1\ pJ$, $\tau_0/\tau_s = 1$. Output chirp decreases for higher medium losses

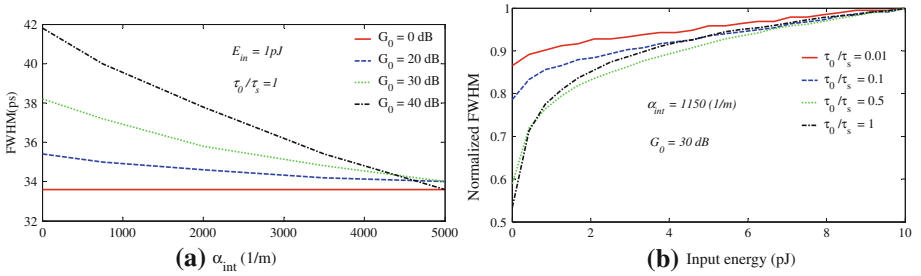

Fig. 4 The output pulse's FWHM, **a** output pulse FWHM for variety of medium loss values, the energy and width of the input pulse are, $E_{in} = 1\ pJ$, $\tau_0/\tau_s = 1$. **b** The Normalized FWHM of the output pulse for variety of input pulse widths values when the input pulse is Gaussian

the SOA's internal loss increases then the FWHM decreases and as the input pulse energy increased, the amplified output pulse broadened more. This is due to the stronger carrier depletion occurred by higher input energy. Furthermore, the output pulses FWHM variations increased due to the wider input pulses. For this case, carriers have enough time to recover the population inversion in conduction band then the output pulse energy and FWHM increased more.

In the following, we analyze the effect of input pulses on the FWM signal. FWM signal pulse has many applications in optical communication systems. Fast and high conversion efficiency converter is a fundamental requirement for future optical communication systems.

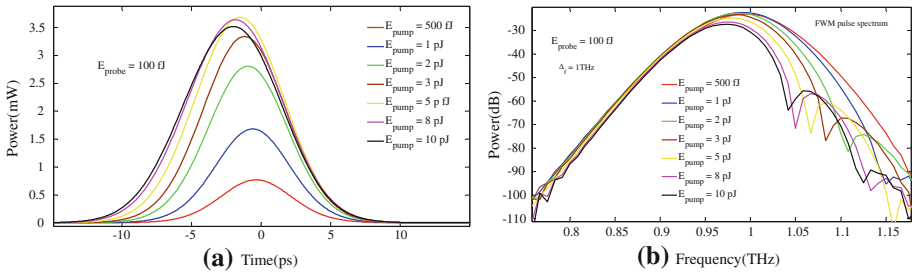

Fig. 5 **a** The waveform of generated FWM pulse for several values of input pump pulse energies. **b** The generated FWM signal spectrum for the waveforms that shown in **a**

An analytical approach is essential in order to design a high efficiency and high-speed FWM conversion devices and clarify the fast FWM interaction processes. When two optical pulses with different central frequencies of f_p(pump) and f_q(probe) are injected into the SOA simultaneously, the FWM signal is generated in the SOA at a frequency of $2f_p - f_q$ (Das et al. 2000). The input probe pulse energy is kept constant at 100 fJ. Figure 5 shows the temporal waveform and spectrum of the FWM signal for several values of input pump pulse energies.

It has shown clearly that the energy of the generated FWM signal increases and its shape becomes wider when the input pump pulse energy increases. The FWM signal intensity is proportional to $I_P^2 I_q$. Here, I_P is the pump intensity and I_q is the probe intensity (Das et al. 2000). Therefore, when the energy of the input pump pulse increases, the FWM signal shape becomes more asymmetric and the spectrum becomes oscillatory due to gain saturation. In the following, we analyze the generated FWM signal characteristics.

Figure 6 illustrates the characteristics of the generated FWM signal that shown in Fig. 5a. It has shown clearly in Fig. 6a that the peak of the FWM pulse experienced a greater shift when the input pump pulse energy increased. This phenomenon is mainly caused by the SPM. As it was clear in Fig. 6b, the FWHM of the FWM signal increases due to the increment of input pump pulse energy. But, for the higher input pump energies carrier depletion effect limit the increasing rate. It is shown in Fig. 6c, the energy of the FWM signal is increasing when the input pump pulse energy is increased. The FWM energy is saturated about 0.03 pJ (or 30 fJ). This comes from gain saturation phenomenon that occurs in SOA for higher input energy regime. In Fig. 6c, we also found that, for such probe pulse, the maximum FWM signal energy is about 0.03 pJ and it cannot be increased by increasing the input pump pulse energy furthermore.

4 Conclusion

In this work, the effects of gain, input pulsewidth, input pulse energy and SOA internal loss are analysed in detail on the output pulse shapes of the SOA. It has shown that the output power decreased when internal loss increased and its shape became broader for a wider input pulsewidth. The output spectrum has experienced a blue shift when the internal loss is increased. It also became broader for the wider input pulsewidth. Furthermore, the chirp imposed to the output pulse was negative for a shorter input pulsewidth and decreased when the internal loss increased. But, for wider input pulsewidth, the chirp experienced both positive and negative values. The output pulsewidth was also sensitive to internal loss, input pulsewidth and gain.

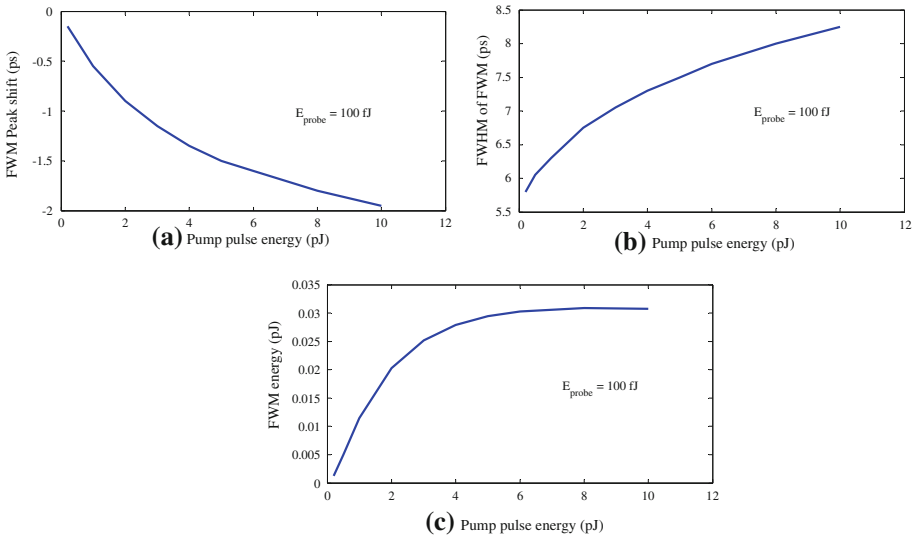

Fig. 6 The characteristics of generated FWM signals that shown in Fig. 5. **a** The peak shift of the generated FWM signal, **b** the FWHM of generated FWM signal and **c** the generated FWM signal energy

It has also depicted that FWHM of the output pulse is inversely proportional to the internal loss. Moreover, when the input pulse energy is increased, the output pulses FWHM value saturated faster. Besides, the effect of input pump pulse energy was also analysed on the FWM characteristics. The FWM signals FWHM, peak shift and energy is increased when the energy of the pump pulse is increased. The energy of the FWM signal remains constant when the SOA is saturated. Based on our simulation results, we conclude that the output pulse characteristics could be modified by controlling the medium internal loss, SOA gain and the pulsewidth and energy of the input pulses.

References

Aghajanpour, H., Ahmadi, V., Razaghi, M.: Ultra-short optical pulse shaping using semiconductor optical amplifier. Opt. Laser Technol. **41**, 654–658 (2009)

Agrawal, G.P., Olsson, N.A.: Self-phase modulation and spectral broadening of optical pulses in semiconductor laser amplifiers. IEEE J. Quantum Electron. **25**(11), 435–442 (1989)

Conte, S.D., de Boor, C.: Elementary Numerical Analysis: An Algorithmic Approach. 3rd edn. McGraw-Hill Book Company Co., Singapore (1981)

Das, N.K., Yamayoshi, Y., Kawaguchi, H.: Analysis of basic four-wave mixing characteristics in a semiconductor optical amplifier by the finite-difference beam propagation method. IEEE J. Quantum Electron. **36**(10), 1184–1192 (2000)

Fernandez, A., Morel, P., Chi, J.W.D.: Temporal and spectral properties of contra-propagating picosecond optical pulses in SOA. Opt. Commun. **259**(2), 465–469 (2006)

Hong, M.Y., Chang, Y.H., Dienes, A., Heritage, J.P., Delfyett, P.J., Dijaili, S., Peterson, F.G.: Femtosecond self- and cross-phase modulation in semiconductor laser amplifiers. IEEE J. Select. Topics Quantum Electron. **2**, 523–539 (1992)

Rafailov, E.U., Loza-Alvarez, P., Sibbett, W., Sokolovskii, G.S., Livshits, D.A., Zhukov, A.E., Ustinov, V.M.: Amplification of femtosecond pulses over by 18 dB in a quantum-dot semiconductor optical amplifier. IEEE Photon. Technol. Lett. **15**(8), 1023–1025 (2003)

Razaghi, M., Ahmadi, M., Connelly, M.J.: Comprehensive finite-difference time-dependent beam propagation model of counterpropagating picosecond pulses in a semiconductor optical amplifier. IEEE J. Light Wave Technol. **27**(15), 3162–3174 (2009)
Razaghi, M., Ahmadi, V., Connelly M.: Femtosecond pulse shaping using counter-propagating pulses in a semiconductor optical amplifier. Opt. Quant Electron, Springer (2009)